Hindawi Publishing Corporation
Discrete Dynamics in Nature and Society
Volume 2008, Article ID 541683, 12 pages
doi:10.1155/2008/541683

*Research Article*

# Chaos in Ecology: The Topological Entropy of a Tritrophic Food Chain Model

**Jorge Duarte,[1,2] Cristina Januário,[1] and Nuno Martins[3]**

[1] *Department of Chemistry, Mathematics Unit, ISEL-High Institute of Engineering of Lisbon, rua Conselheiro Emídio Navarro 1, 1959-007 Lisbon, Portugal*
[2] *Research Centre in Mathematics and Applications (CIMA), University of Evora, rua Romão Ramalho 59, 7000-671 Evora, Portugal*
[3] *Department of Mathematics, Centre of Mathematical Analysis, Geometry and Dynamical Systems, Instituto Superior Técnico (IST), Technical University of Lisbon, rua Rovisco Pais 1, 1049-001 Lisbon, Portugal*

Correspondence should be addressed to Jorge Duarte, jduarte@deq.isel.ipl.pt

Received 9 December 2007; Accepted 18 June 2008

Recommended by A. Reggiani

An ecosystem is a web of complex interactions among species. With the purpose of understanding this complexity, it is necessary to study basic food chain dynamics with preys, predators and superpredators interactions. Although there is an elegant interpretation of ecological models in terms of chaos theory, the complex behavior of chaotic food chain systems is not completely understood. In the present work we study a specific food chain model from the literature. Using results from symbolic dynamics, we characterize the topological entropy of a family of logistic-like Poincaré return maps that replicates salient aspects of the dynamics of the model. The analysis of the variation of this numerical invariant, in some realistic system parameter region, allows us to quantify and to distinguish different chaotic regimes. This work is still another illustration of the role that the theory of dynamical systems can play in the study of chaotic dynamics in life sciences.



## 1. Motivation and preliminaries

The detailed examination of food chain dynamics is crucial to the study of important ecological systems. Basic food chains can be thought as fundamental "building blocks" of an ecosystem. The chaos theory, which has always intertwinedwith complex population dynamics since its inception, is accepted as an important part of a paradigm by which ecological complexity can be understood.

A compelling reason to study *ecochaos*, beside the challenging mathematical problems that occur in this context, is due to a recent discovery (which may have important management implications) that the average superpredator biomass in various tritrophic food chain models is maximum at the onset of chaos (see [1, 2], and references therein).

The main dynamical features of the well-known Lotka-Volterra models for two species interactions, which are spatially homogeneous and time autonomous, are steady states and limiting cycles. However, models for tritrophic food chains are extremely rich in complex dynamics. The strong nonlinearity and high dimensionality of the phase space are a significant obstacles in understanding the qualitative behavior of such systems.

The dynamical principles and mechanisms underlying the chaotic food chain behavior can be analyzed with comprehensive studies of low-dimensional systems, which emerge from the food chain models. Indeed, we can gain some important qualitative insights by studying representative return maps, considered as one-dimensional interval maps.

The aim of this work is to provide a contribution for the detailed analysis of the chaotic behavior of the time-diversified Rosenzweig-MacArthur tritrophic model, which is cast as a singularly perturbed system. More precisely, using results of symbolic dynamics theory, we compute the topological entropy of a family of logistic-like Poincaré return maps (with the shape of a unimodal map) presented in [4], which incorporates fundamental dynamical properties of the three-dimensional attractor. This measure of the amount of chaos in a dynamical system is the most important numerical invariant related to the orbit growth and its variation with particular parameters gives us a finer distinction between states of complexity.

For the sake of clarity, the next paragraph begins with an overview of the food web model considered (the reader is referred to [4]).

## 2. Description of the model

The Rosenzweig-MacArthur model for tritrophic food chains is given by the following differential system:

$$\begin{aligned}
\dot{X} &= X\left(r - \frac{rX}{K} - \frac{p_1 Y}{H_1 + X}\right),\\
\dot{Y} &= Y\left(\frac{c_1 X}{H_1 + X} - d_1 - \frac{p_2 Z}{H_2 + Y}\right),\\
\dot{Z} &= Z\left(\frac{c_2 Y}{H_2 + Y} - d_2\right).
\end{aligned} \tag{2.1}$$

It is composed of a logistic prey $X$, a predator $Y$, and a top predator $Z$. The model assumes *predator/top predator* responses that reflect the more realistic situations in the saturation capture rate of *prey by predator/predator by top predator*.

In order to simplify the mathematical analysis, it is appropriate to nondimensionalize the previous equations (2.1) so that the scaled system contains a minimal number of parameters. We use the same scaling of variables and parameters as in [4],

$$\begin{gathered}
t \longrightarrow c_1 T, \qquad x \longrightarrow \frac{1}{K} X, \qquad y \longrightarrow \frac{p_1}{rK} Y, \qquad z \longrightarrow \frac{p_2 p_1}{c_1 rK} Z,\\
\zeta = \frac{c_1}{r}, \qquad \epsilon = \frac{c_2}{c_1}, \qquad \beta_1 = \frac{H_1}{K}, \qquad \beta_2 = \frac{H_2}{Y_0}, \quad \text{with } Y_0 = \frac{rK}{p_1},\\
\delta_1 = \frac{d_1}{c_1}, \qquad \delta_2 = \frac{d_2}{c_2}.
\end{gathered} \tag{2.2}$$

This procedure leads to the following dimensionless form

$$\begin{aligned}\zeta\,\dot{x} &= x\left(1-x-\frac{y}{\beta_1+x}\right),\\ \dot{y} &= y\left(\frac{x}{\beta_1+x}-\delta_1-\frac{z}{\beta_2+y}\right),\\ \dot{z} &= \epsilon z\left(\frac{y}{\beta_2+y}-\delta_2\right).\end{aligned} \tag{2.3}$$

In the context of ecology, the parameters have the following definitions:

(i) $\zeta = c_1/r$, where $c_1$ is the maximum per capita growth rate of the predator and $r$ is the maximum per capita growth rate for the prey;

(ii) $\epsilon = c_2/c_1$, where $c_2$ is the maximum per capita growth rate of the top predator and $c_1$ is the maximum per capita growth rate for the predator;

(iii) $\beta_1$ is the dimensionless semisaturation constant measured against prey's carrying capacity;

(iv) $\beta_2$ is the dimensionless semisaturation constant for the predator, measured against its predation capacity;

(v) $\delta_1 = d_1/c_1$, where $d_1$ is the per capita natural death rate of the predator and $c_1$ is the maximum per capita growth rate for the predator;

(vi) $\delta_2 = d_2/c_2$, where $d_2$ is the per capita natural death rate of the top predator and $c_2$ is the maximum per capita growth rate for the top predator.

As in [4], we assume throughout that

$$0<\beta_1<1, \qquad 0<\beta_2<1, \tag{2.4}$$

which can be interpreted to mean that both the predator and the superpredator are good hunters. We also assume throughout that

$$0<\delta_1=\frac{d_1}{c_1}<1, \qquad 0<\delta_2=\frac{d_2}{c_2}<1. \tag{2.5}$$

This is in fact a default assumption because the condition of either $\delta_i > 1$ $(i = 1,2)$ would lead to the collapse of the tritrophic food chain. More specifically, with $d_1 > c_1$, the predator dies out faster than it can reproduce even at its maximum reproduction rate. With $d_2 > c_2$, the top predator must die out by the same reasoning. In both cases, we would have a trivial tritrophic food chain, whose dynamics is entirely understood.

Under the "trophic time diversification hypothesis," which states that *the maximum per capita growth rate decreases from bottom to top along the food chain, namely,*

$$r > c_1 > c_2 > 0 \tag{2.6}$$

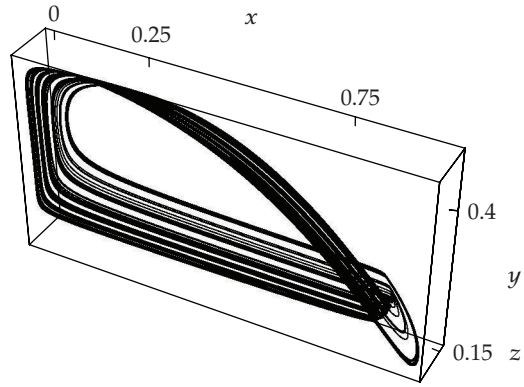


**Figure 1:** Solution visualized as a trajectory in the three-dimensional space for $\epsilon = 0.4$ and $\delta_2 = 0.65$.

or equivalently

$$0 < \zeta \ll 1, \qquad 0 < \epsilon < 1. \tag{2.7}$$

Equation (2.3) become a singularly perturbed system of three-time scales. The rates of change for the prey, predator, and top predator are fast, intermediate, and slow, respectively. From the ecological point of view, it means that the prey reproduces faster than the predator which in turn reproduces faster than the top predator.

## 3. Unimodal return maps. Symbolic dynamics, topological entropy, and chaos

As we mentioned before, this paper aims to address a study of the topological entropy of a family of logistic-like Poincaré return maps associated to the model (2.3). The existence of these maps, for some system realistic parameter region (see region $\Omega$ in Figure 8 represented below), was demonstrated in [4] using a geometric method of singular perturbations, which have proved to be extremely effective for ecological models (see [4–7]).

For numerical investigation, we will use throughout

$$\zeta = 0.1, \qquad \beta_1 = 0.3, \qquad \beta_2 = 0.1, \qquad \delta_1 = 0.2, \tag{3.1}$$

and consider $\epsilon$ and $\delta_2$ as control parameters. As we saw earlier, the parameter $\epsilon$ is the reproduction rate ratio of the top predator over the predator and the parameter $\delta_2$ is the ratio of the per capita natural death rate of the top predator over its reproduction rate.

### *3.1. Return maps*

Using numerical integration of the system (2.3), we can gain some insights about the geometry of the trajectories in the long run. After an initial transient, a structure emerges when the solution $(x(t), y(t), z(t))$ is visualized as a trajectory in three-dimensional space (see Figure 1). The projection of the three-dimensional trajectory onto a two-dimensional plane is exhibited in Figure 2.

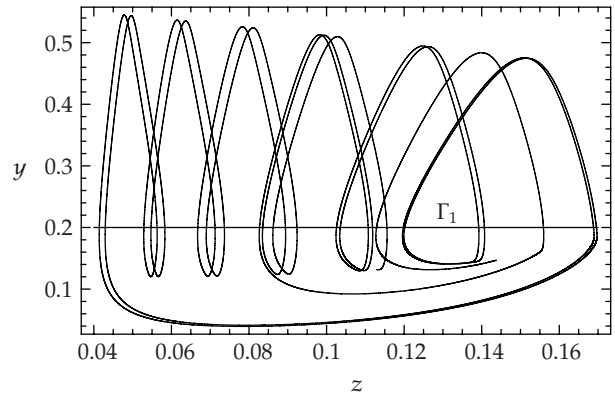


**Figure 2:** Projection of the three-dimensional trajectory onto the $zy$-plane for $\epsilon = 0.4$ and $\delta_2 = 0.65$.

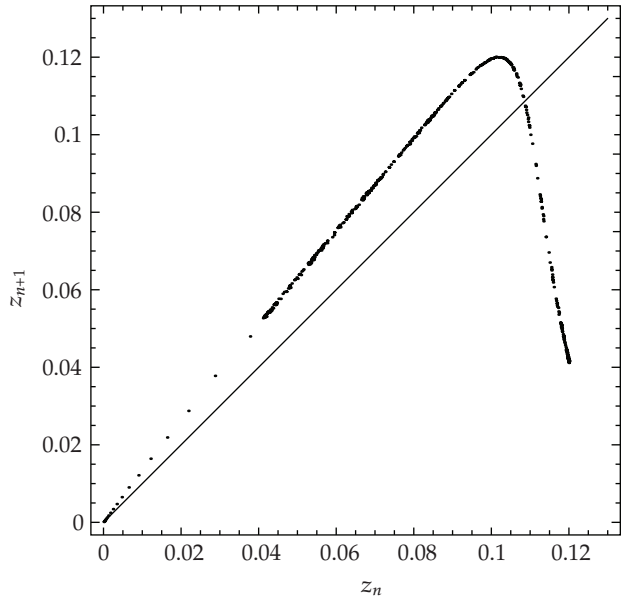


**Figure 3:** The iterated map for $\epsilon = 0.4$ and $\delta_2 = 0.65$.

With the purpose of understanding the main features of the three-dimensional flow, we can use the Poincaré map technique to reduce the dimensionality of the phase space and so make the analysis simpler. Now we briefly describe the construction of a Poincaré map.

Consider an $n$-dimensional system $d\mathbf{x}/dt = \mathbf{f}(\mathbf{x})$. Let $P$ be an $(n-1)$-dimensional surface, called a Poincaré section. $P$ is required to be transverse to the flow. The Poincaré map $F$ is a map from $P$ to itself, obtained by following trajectories from one intersection with $P$ to the next. If $x_n \in P$ denotes the $n$th intersection, then the Poincaré map is defined by $x_{n+1} = F(x_n)$. In our particular case, we have a system with three dynamical variables and we consider a Poincaré plane of the form $y = k (k \in \mathbb{R})$, namely, $\Gamma_1 : y = 0.2$ (see Figure 2). After allowing the initials to decay, we record the successive intersections of the trajectory with the plane, which are specified by two coordinates $x_n$ and $z_n$. The logistic-like iterated map of Figure 3 consists of pairs $(z_n, z_{n+1})$, obtained from the successive second coordinates of the

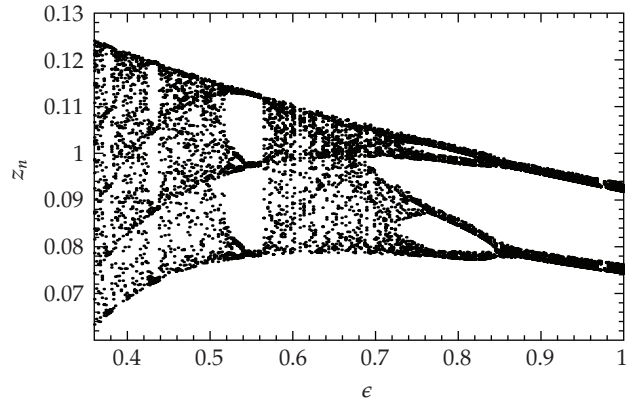


**Figure 4:** Bifurcation diagram for $z_n$ as a function of $\varepsilon$, with $\delta_2 = 0.662$ and $\epsilon \in [0.36, 1.0[$.

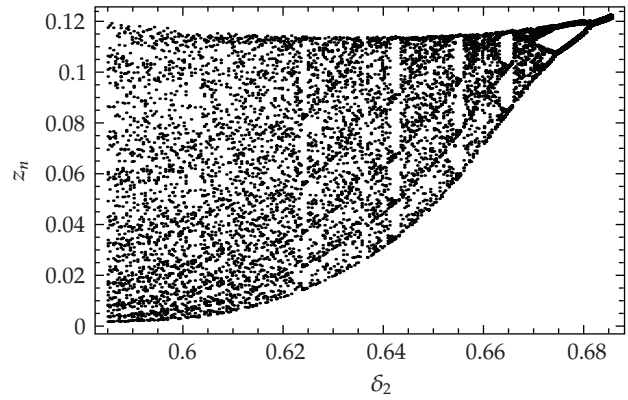


**Figure 5:** Bifurcation diagram for $z_n$ as a function of $\delta_2$, with $\epsilon = 0.5$ and $\delta_2 \in [0.585, 0.686[$.

points defined by the Poincaré map. The obtained iterated map dynamically behaves like a unimodal map (family of continuous maps on the interval with two monotonic subintervals and one turning point).

In order to see the long term behavior for different values of the parameters at once, we plot typical bifurcation diagrams. The dynamics bifurcate into stable equilibria with the increase in the parameters $\epsilon$ and $\delta_2$ (see Figures 4 and 5).

At this point, we are in a position to devote our attention to the study of the topological entropy of the logistic-like return maps using results of symbolic dynamics theory.

### *3.2. Symbolic dynamics, topological entropy, and chaos*

In this paragraph, we describe techniques of symbolic dynamics, in particular some results concerning to Markov partitions associated to unimodal maps. For more details see [8–10].

A unimodal map $f$ on the interval $I = [a, b]$ is a 2-piecewise monotone map with one critical point $c$. Thus $I$ is subdivided into the following sets:

$$I_L = [a, c[, \qquad I_C = \{c\}, \qquad I_R = ]c, b], \tag{3.2}$$

in such way that the restriction of $f$ to interval $I_L$ is strictly increasing and the restriction of $f$ to interval $I_R$ is decreasing (see Figure 3). Each of such maximal intervals on which the function $f$ is monotone is called a *lap* of $f$, and the number $\ell = \ell(f)$ of distinct laps is called the lap number of $f$. Beginning with the critical point of $f$, $c$ (relative extremum), we obtain the orbit

$$O(c) = \{x_i : x_i = f^i(c),\ i \in \mathbb{N}\}. \tag{3.3}$$

With the purpose of studying the topological properties, we associate to the orbit $O(c)$ a sequence of symbols, itinerary $(i(x))_j = S = S_1S_2 \ldots S_j \ldots$, where $S_j \in \mathcal{A} = \{L, C, R\}$ and

$$\begin{aligned} S_j &= L, \quad \text{if } f^j(x) < c, \\ S_j &= C, \quad \text{if } f^j(x) = c, \\ S_j &= R, \quad \text{if } f^j(x) > c. \end{aligned} \tag{3.4}$$

The turning point $c$ plays an important role. The dynamics of the interval is characterized by the symbolic sequence associated to the critical point orbit. When $O(c)$ is a $k$-periodic orbit, we obtain a sequence of symbols that can be characterized by a block of length $k$, the kneading sequence $S^{(k)} = S_1S_2 \ldots S_{k-1}C$.

We introduce, in the set of symbols, an order relation $L < C < R$. The order of the symbols is extended to the symbolic sequences. Thus, for two of such sequences $P$ and $Q$ in $\mathcal{A}^{\mathbb{N}}$, let $i$ be such that $P_i \neq Q_i$ and $P_j = Q_j$ for $j < i$. Considering the $R$-parity of a sequence, meaning odd or even number of occurrence of a symbol $R$ in the sequence, if the $R$-parity of the block $P_1 \ldots P_{i-1} = Q_1 \ldots Q_{i-1}$ is even, we say that $P < Q$, if $P_i < Q_i$. And if the $R$-parity of the same block is odd, we say that $P < Q$, if $P_i > Q_i$. If no such index $i$ exists, then $P = Q$.

The ordered sequence of elements $x_i$ of $O(c)$ determines a partition $\mathcal{P}^{(k-1)}$ of the interval $I = [f^2(c), f(c)] = [x_2, x_1]$ into a finite number of subintervals labeled by $I_1, I_2, \ldots, I_{k-1}$. To this partition, we associate a $(k-1) \times (k-1)$ transition matrix $M = [a_{ij}]$ with

$$a_{ij} = \begin{cases} 1 & \text{if } I_j \subset f(I_i), \\ 0 & \text{if } I_j \not\subseteq f(I_i). \end{cases} \tag{3.5}$$

Now we consider the topological entropy. As we pointed out before, this important numerical invariant is related to the orbit growth and allows us to quantify the complexity of the phenomenon. It represents the exponential growth rate for the number of orbit segments distinguishable with arbitrarily fine but finite precision. In a sense, the topological entropy describes in a suggestive way the total exponential complexity of the orbit structure with a single number.

A definition of chaos in the context of one-dimensional dynamical systems states that a dynamical system is called chaotic if its topological entropy is positive. Thus, the topological entropy can be computed to express whether a map has chaotic behavior, as we can see in [11, 12]. In these references, Glasner and Weiss, in a discussion of Devaney's definition (of chaos), proposed positive entropy as a strong property for the characterization of complex dynamical systems, more precisely, as the essential criterium of chaos. Important results were constructed using this property (see [13, 14]).

The topological entropy of a unimodal interval map $f$, denoted by $h_{\text{top}}(f)$, is given by

$$h_{\text{top}}(f) = \log \lambda_{\max}\left(M(f)\right) = \log s(f), \tag{3.6}$$

where $\lambda_{\max}(M(f))$ is the spectral radius of the transition matrix $M(f)$ and $s(f)$ is the growth rate,

$$s(f) = \lim_{k\to\infty} \sqrt[k]{\ell\left(f^k\right)}, \tag{3.7}$$

of the lap number of $f^k$ ($k$th-iterate of $f$) (see [10, 15, 16]). In summary, for each value of the parameter, the computation begins with the symbolic codification of the critical point orbits which determines a Markov partition of the interval. Then, we compute the transition matrix induced by the interval map on the Markov partition. Finally, the topological entropy is given by the logarithm of the highest eigenvalue of this transition matrix.

In order to illustrate the outlined formalism about the computation of the topological entropy, we discuss the following example.

*Example 3.1.* Let us consider the map of Figure 3. The orbit of the turning point defines the period-6 kneading sequence $(RLLLLC)^\infty$. Putting the orbital points in order we obtain

$$x_2 < x_3 < x_4 < x_5 < x_0 < x_1. \tag{3.8}$$

The corresponding transition matrix is

$$M(f) = \begin{bmatrix} 0 & 1 & 0 & 0 & 0 \\ 0 & 0 & 1 & 0 & 0 \\ 0 & 0 & 0 & 1 & 0 \\ 0 & 0 & 0 & 0 & 1 \\ 1 & 1 & 1 & 1 & 1 \end{bmatrix}, \tag{3.9}$$

which has the characteristic polynomial

$$p(\lambda) = \det\left(M(f) - \lambda I\right) = 1 + \lambda + \lambda^2 + \lambda^3 + \lambda^4 - \lambda^5. \tag{3.10}$$

The growth number $s(f)$ (the spectral radius of matrix $M(f)$) is $1.96595\ldots$. Therefore, the value of the topological entropy can be given by

$$h_{\text{top}}(f) = \log s(f) = 0.675975\ldots. \tag{3.11}$$

Several situations of the variation of the topological entropy with each of the parameters are plotted in Figures 6 and 7. We emphasize that the logistic-like family of Poincaré return maps associated to the Rosenzweig-MacArthur model for tritrophic chains exhibit positive topological entropy, which is a signature of its chaotic behavior. Indeed, the

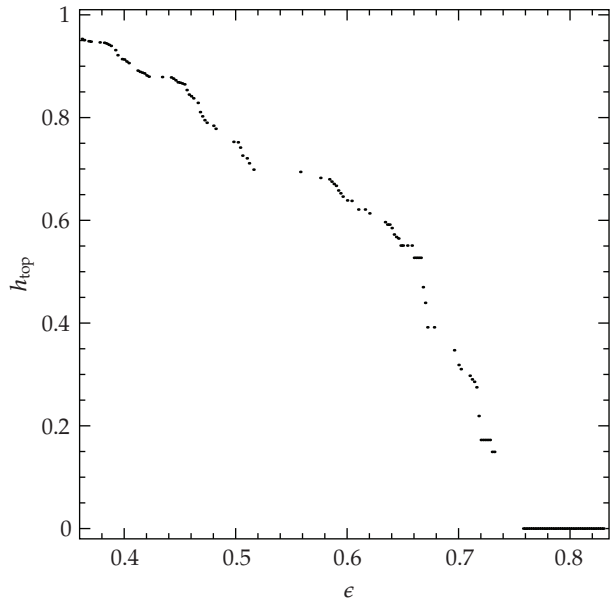


**Figure 6:** Variation of the topological entropy for $\epsilon \in [0.36, 1.0[$, with $\delta_2 = 0.662$.

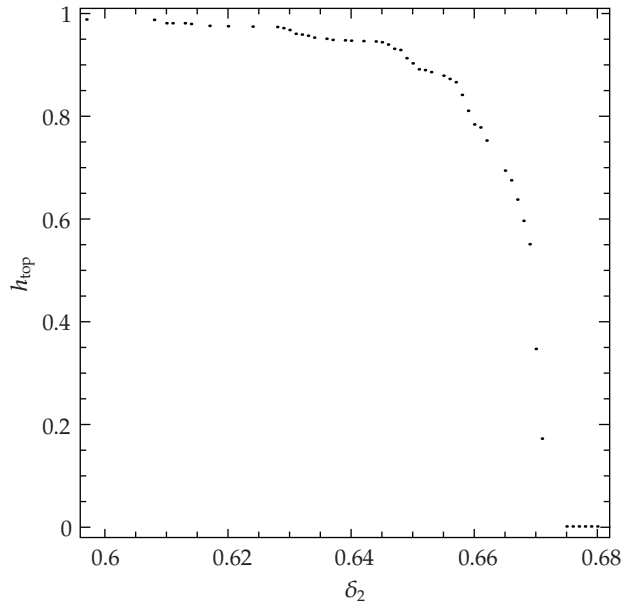


**Figure 7:** Variation of the topological entropy for $\delta_2 \in [0.585, 0.686]$, with $\epsilon = 0.5$.

consideration of a Poincaré section of the type $y = k$ led us to identify a large region of the parameter space, associated to logistic-like maps, where chaos occurs.

It is interesting to notice that with the study of the kneading sequences it is possible to represent the curves, in the region $\Omega$ of the parameter space, corresponding to the periodic orbits of the turning point $C$. The diagram of Figure 8 shows how the periods ($n \leq 5$)

**Table** 1

| Kneading sequences | Characteristic polynomial | Topological entropy |
|---|---|---|
| *RC* | $1 - t$ | 0 |
| *RLRC* | $-1 + t + t^2 - t^3$ | 0 |
| *RLRRC* | $-1 + t - t^2 - t^3 + t^4$ | 0.414013... |
| *RLC* | $-1 - t + t^2$ | 0.481212... |
| *RLLRC* | $1 - t - t^2 - t^3 + t^4$ | 0.543535... |
| *RLLC* | $1 + t + t^2 - t^3$ | 0.609378... |
| *RLLLC* | $-1 - t - t^2 - t^3 + t^4$ | 0.656256... |

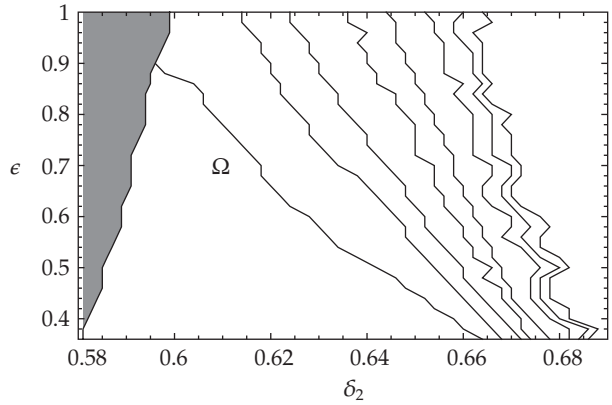


**Figure 8:** Periodic orbits ($n \leq 5$) of the turning point $C$ in the $\Omega$ region. From right to left, the corresponding kneading sequences are as follows: $C^\infty$, $(RC)^\infty$, $(RLRC)^\infty$, $(RLRRC)^\infty$, $(RLC)^\infty$, $(RLLRC)^\infty$, $(RLLC)^\infty$, and $(RLLLC)^\infty$. The parameter values in the grey region do not correspond to unimodal maps and are beyond the scope of our study.

are organized throughout the region $\Omega$ of the parameter space considered (whose pairs of values $(\delta_2, \epsilon)$ correspond to logistic-like Poincaré return maps). From right to left in Figure 8, the corresponding kneading orbits are as follows: 1-period—$C^\infty$, 2-period—$(RC)^\infty$, 4-period—$(RLRC)^\infty$, 5-period—$(RLRRC)^\infty$, 3-period—$(RLC)^\infty$, 5-period—$(RLLRC)^\infty$, 4-period—$(RLLC)^\infty$, and 5-period—$(RLLLC)^\infty$. The parameter space ordering of the kneading sequences leads to the identification of different levels for the topological entropy, which remains constant over each curve. Table 1 represents some kneading sequences and the corresponding topological entropy.This is an example of how our understanding of the parameter space can be enhanced by the techniques of symbolic dynamics.

## 4. Final considerations

In this paper, we have provided new insights into the study of a very well-known model in the field of theoretical ecology: the Rosenzweig-MacArthur model for tritrophic food chains. In the available literature, the detailed examination of this remarkable model involves many different issues, both in the biological and mathematical domains, and its scientific investigation is still an active research area. As pointed out in the introduction, a plausible and compelling motive to study chaos in ecology is due to the principle (which may have a direct biological relevance and significant management implications) that the average top

predator biomass, in various tritrophic food chain models, is maximum at the onset of chaos. From the point of view of mathematics, chaos in food chain models is not clearly understood. Indeed, the first theorem on the existence of chaotic food chain dynamics was recently obtained in [4]. The characterization and analysis of chaos generating mechanisms for the Rosenzweig-MacArthur tritrophic food chain model are one of the recent significant achievements in mathematics applied to ecology (see [4–6, 17]). These studies proved the existence of different one-dimensional Poincaré return maps generated by the model and left open a collection of questions pertaining to chaotic attractors in terms of symbolic dynamics and various measurements of complexity (see [5]). In this context, the work carried out in the present article addresses a contribution for the comprehensive mathematical study of the chaotic behavior associated to a specific class of one-dimensional return maps (see [18], for the analysis of a different class of maps).

In the field of life sciences, where quantitatively predictive theories are rare, the use of powerful tools for the analysis of dynamic models, such as the symbolic dynamics theory, stands out to be extremely effective for the computation of an important numerical invariant related to the exponential orbit growth—the topological entropy. In fact, a rigorous study of the iterated maps, that incorporate the salient dynamical properties of the system, became possible analyzing the variation of this measure of complexity with the two control parameters $\epsilon$ and $\delta_2$. Our analysis reveals that when the reproduction rate of the top predator and the reproduction rate of the predator become closer (which means an increase in $\epsilon$), the topological entropy decreases. In a similar way, when the per capita natural death rate of the top predator becomes closer to its reproduction rate (which means an increase in $\delta_2$), the topological entropy also decreases. Therefore, high values of these control parameters tend to stabilize the food chain. To each value of these control parameters corresponds a value of the topological entropy which is a quantifier for the complex orbit structure and an attribute efficiently used to identify different chaotic states.

The representation of the isentropic curves (corresponding to the periodic orbits of the turning point $c$) in the region $\Omega$ allowed us to introduce the parameter space ordering of the dynamics. In fact, this construction gives insights about the behavior of the topological entropy in all the parameter space considered.

Indeed, the family of maps associated to the model exhibits positive topological entropy, which demonstrates its chaotic nature. The techniques of symbolic dynamics allowed us to quantify the orbit complexity and to distinguish different chaotic regimes (extracting order from chaos) in a significant region of the parameter space.

## Acknowledgments

The authors would like to thank Professor Bo Deng for his enlightenments and valuable information. This work is partially supported by ISEL and CIMA-UE.

## References

[1] O. De Feo and S. Rinaldi, "Yield and dynamics of tritrophic chains," *The American Naturalist*, vol. 150, pp. 328–345, 1997.
[2] S. Rinaldi and O. De Feo, "Top-predator abundance and chaos in tritrophic food chains," *Ecology Letters*, vol. 2, no. 1, pp. 6–10, 1999.
[3] M.L. Rosenzweig and R.H. MacArthur, "Graphical representation and stability conditions of predator-prey interactions," *The American Naturalist*, vol. 97, pp. 209–223, 1963.
[4] B. Deng, "Food chain chaos due to junction-fold point," *Chaos*, vol. 11, no. 3, pp. 514–525, 2001.

[5] B. Deng and G. Hines, "Food chain chaos due to Shilnikov's orbit," *Chaos*, vol. 12, no. 3, pp. 533–538, 2002.
[6] B. Deng and G. Hines, "Food chain chaos due to transcritical point," *Chaos*, vol. 13, no. 2, pp. 578–585, 2003.
[7] W. Liu, D. Xiao, and Y. Yi, "Relaxation oscillations in a class of predator-prey systems," *Journal of Differential Equations*, vol. 188, no. 1, pp. 306–331, 2003.
[8] J. P. Lampreia and J. Sousa Ramos, "Symbolic dynamics of bimodal maps," *Portugaliae Mathematica*, vol. 54, no. 1, pp. 1–18, 1997.
[9] B.-L. Hao and W.-M. Zheng, *Applied Symbolic Dynamics and Chaos*, vol. 7 of *Directions in Chaos*, World Scientific, River Edge, NJ, USA, 1998.
[10] J. Milnor and W. Thurston, "On iterated maps of the interval," in *Dynamical Systems*, vol. 1342 of *Lecture Notes in Mathematics*, pp. 465–563, Springer, Berlin, Germany, 1988.
[11] E. Glasner and B. Weiss, "Sensitive dependence on initial conditions," *Nonlinearity*, vol. 6, no. 6, pp. 1067–1075, 1993.
[12] F. Blanchard, "Topological chaos: what may this mean?" http://arxiv.org/abs/0805.0232v1.
[13] R. Gilmore and M. Lefranc, *The Topology of Chaos: Alice in Stretch and Squeezelan*, John Wiley & Sons, New York, NY, USA, 2002.
[14] S. Ruette, "Chaos for continuous interval maps—a survey of relationship between the various sorts of chaos," preprint, http://www.math.u-psud.fr/~ruette/publications.html.
[15] J. P. Lampreia and J. Sousa Ramos, "Computing the topological entropy of bimodal maps," in *European Conference on Iteration Theory (Caldes de Malavella, 1987)*, pp. 431–437, World Scientific, Teaneck, NJ, USA, 1989.
[16] M. Misiurewicz and W. Szlenk, "Entropy of piecewise monotone mappings," *Studia Mathematica*, vol. 67, no. 1, pp. 45–63, 1980.
[17] B. Deng, "Food chain chaos with canard explosion," *Chaos*, vol. 14, no. 4, pp. 1083–1092, 2004.
[18] J. Duarte, C. Januário, and N. Martins, "Topological invariants in the study of a chaotic food chain system," *Chaos*, vol. 18, no. 2, Article ID 023109, 9 pages, 2008.